Journal of the Korean Physical Society, Vol. 48, No. 3, March 2006, pp. 446∼450

Coexistence of the Kondo and the Superconducting Proximity Effects in AuFe/Al Loops

Jonghwa EOM*
Department of Physics, Sejong University, Seoul 143-747

Yun-Sok SHIN, Hu-Jong LEE and Dong-Kun KIE
Department of Physics, Pohang University of Science and Technology, Pohang 790-784

Taegon KIM and Jonghan SONG
Advanced Analysis Center, Korea Institute of Science and Technology, Seoul 130-650

(Received 14 November 2005)

We present measurements of the transport properties of hybrid loops consisting of a Kondo AuFe film and a superconducting Al film. The temperature dependence of the resistance and the significant phase modulation of the resistance indicate the existence of the superconducting proximity effect over the range of ∼0.5 μm in AuFe wires with Fe concentrations of 26 ppm and 70 ppm. The magnetoresistance oscillation of AuFe/Al hybrid loops shows a reentrant behavior in temperature. The electronic phase coherence in the Kondo AuFe wires has been further confirmed by the weak localization measurement.

PACS numbers: 74.45.+c, 72.15.Qm, 73.23.-b
Keywords: Superconducting proximity effect, Kondo effect, Andreev interferometer

I. INTRODUCTION

In a normal metal in contact with a superconductor, the existence of electronic phase coherence allows the superconducting order parameter to propagate into the normal metal within a certain range, leading to the superconducting proximity effect. The length scale for the range of the superconducting proximity effect is determined by the thermal length, L_T, in a nonmagnetic metal, which easily reaches a few μm below $T = 1$ K. This leads to a significant change in the resistivity of a mesoscopic metal film near a superconductor below the superconducting transition temperature [1]. In a recent article [2,3], the temperature-dependent resistivity of 100-ppm AuFe wires showed a possible significant contribution from the superconducting proximity effect, even in strong spin scattering. In addition, a possible coexistence of the Kondo effect and the superconducting proximity effect has been suggested in systems where the Kondo temperature T_K is comparable to the superconducting gap energy [4, 5]. The existence of the superconducting proximity effect in magnetic metals, however, is questionable because Cooper pairs of an s-wave nature experience strong spin-flip scattering. Even in dilute magnetic metallic systems (Kondo systems), spin-flip scattering is strong at low temperatures.

Since a long-range anomalous temperature dependence in the resistivity of mesoscopic Co/Al hybrid structures was reported [6], the existence of the superconducting proximity effect in magnetic systems has been a subject of continuing experimental and theoretical interest [7–10]. For ferromagnetic metals, the proximity effect extends only to a distance determined by the exchange field energy, $\xi_{ex} = \sqrt{\hbar D/k_B T_{Curie}}$, where T_{Curie} is the Curie temperature of the ferromagnetic metal. This length scale is a few nm at most; hence, no significant proximity effect is expected in the transport properties. To explain the observed anomalous behavior in the temperature dependence of the resistivity in ferromagnetic metal/supercondcutor systems, Belzig *et al.* proposed an interplay between Andreev reflection and spin accumulation at the ferromagnetic metal/superconductor interface [9]. On the other hand, Bergeret *et al.* proposed the existence of a triplet superconducting pair correlation in ferromagnetic metals [10].

In this paper, we report observation of the superconducting proximity effect in a mesoscopic Kondo system, to which superconducting wires were connected through clean interface with very low resistance. The Kondo systems were AuFe wires with Fe concentrations of 26 ppm and 70 ppm, and Al film was used for a superconductor. The Kondo effect was confirmed by observ-

*E-mail: eom@sejong.ac.kr; Fax: +82-2-461-9356

ing the logarithmic temperature dependence of the resistivity at low temperatures. In addition, the superconducting proximity effect was observed in the AuFe wire when the temperature, T, was lowered below the superconducting transition temperature, T_c, of the Al films. The resistance started to drop as the samples were cooled through T_c. The change in the relative resistance ($\Delta R/R$) depended on the Fe concentration of the AuFe wire. While the resistance of the Au/Al loop structure continuously decreased down to the lowest temperature, the resistance of the AuFe/Al loop structures showed a non-monotonic behavior, which resulted from an interplay between the Kondo effect and the superconducting proximity effect. Phase-coherent transport under the superconducting proximity effect was confirmed by observing magnetoresistance oscillations of the AuFe/Al loop structures for both Fe concentrations of 26 ppm and 70 ppm.

II. EXPERIMENTS AND DISCUSSION

The samples used in this experiment were patterned by using multilevel electron-beam lithography and a lift-off process. In the first lithography step, a 500-Å-thick film was deposited by thermal evaporation of 99.999 %-pure Au. After lift-off, the pure Au film was implanted with Fe ions to concentrations of 26 ppm and 70 ppm [11], which were estimated subsequently from the slope of the temperature-dependent resistivity of the AuFe control wires [12]. In the second lithography step, a 1200-Å-thick Al film was deposited to make hybrid structures in the middle of the sample wires, the length of which was $\sim$4.7 μm for both samples. The resistance of the interface between the AuFe film and the Al film, obtained by using the contact lines that were connected to the Al arm of sample A, was 0.4 Ω at $T = 1$ K. Figure 1 shows typical scanning electron micrographs of the two hybrid samples. Figures 1(a) and 1(b) are AuFe/Al loop structures consisting of a 26-ppm AuFe wire (sample A) and a 70-ppm AuFe wire (sample B), respectively. A pure Au/Al hybrid loop of the same structure as sample B was also fabricated in a simultaneous process and was measured for comparison.

The samples were measured in a dilution refrigerator by using standard lock-in techniques with a four-terminal ac resistance bridge. The four-terminal measurement configurations for the two samples are described in Figures 1(a) and 1(b). The resistivity of the 26-ppm AuFe wire for sample A was 1.37 $\mu\Omega$cm at 4.2 K and its thermal length, $L_T = \sqrt{\hbar D/k_B T}$, was $\sim 0.47/\sqrt{T[K]}$ μm at a temperature T. Here, D is the diffusion constant. The resistivity of the 70-ppm AuFe wire for sample B was 1.1 $\mu\Omega$cm at 4.2 K, and L_T was $\sim 0.52/\sqrt{T[K]}$ μm.

Figure 2 shows the zero-magnetic-field temperature-dependent resistivity of meander-type AuFe control wires (26 ppm and 70 ppm). The AuFe control wires were co-fabricated with samples A and B, respectively, by using simultaneous lithographical processes and Fe implantation. The 26-ppm AuFe (70-ppm AuFe) control wire was 0.14-μm (3.0-μm) wide and 374-μm (1206-μm) long. At temperatures above $\sim$9.0 K, where the phonon contribution dominates the resistivity, the resistivity of the AuFe wire decreased as T was lowered. For T below $\sim$9.0 K, the resistivity $\rho(T)$ of the AuFe control wires showed the Kondo effect.

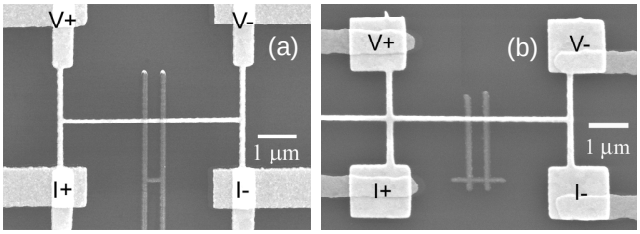

Fig. 1. Sample geometry. (a) Scanning electron micrograph of sample A, which consists of a 26-ppm AuFe film and an Al film. A horse-shoe-type Al wire makes a hybrid loop at the center of a AuFe wire. The AuFe wire appears brighter than the Al wire. (b) Scanning electron micrograph of sample B, which consists of a 70-ppm AuFe film and an Al film.

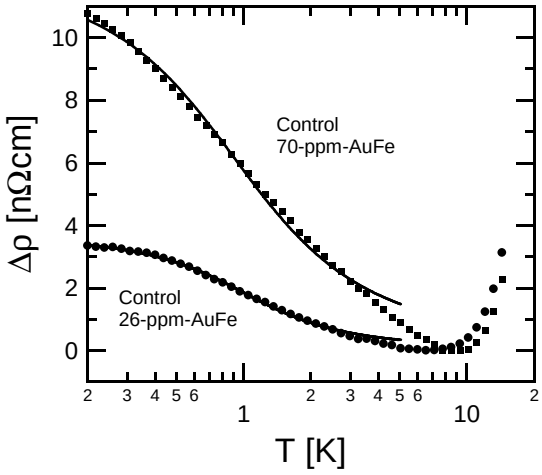

Fig. 2. Temperature dependence of the resistivity of a meander-type 26-ppm AuFe control wire (closed circle) and a meander-type 70-ppm AuFe control wire (closed square) in zero magnetic field. The resistivities at 9.0 K are 1.4 $\mu\Omega$cm, (0.57 $\mu\Omega$cm) for the 26-ppmm AuFe (70-ppm AuFe) control wire. The solid lines represent the best fits to the Hamann function.

For the resistivity of dilute magnetic alloys, the lowest-order calculation in the second Born approximation yields a term linear in $\log T$. When the temperature is comparable to the Kondo temperature, T_K, the purely logarithmic dependence is slightly modified. Considering the nature of the spin correlations over the temperature range above and below T_K, Hamann derived a specific functional form for the Kondo contribution to $\rho(T)$ [13]. Each solid line in Figure 2 represents a fit to the Hamann function with $T_K = 0.99$ K (0.90 K) for the 26-ppm AuFe

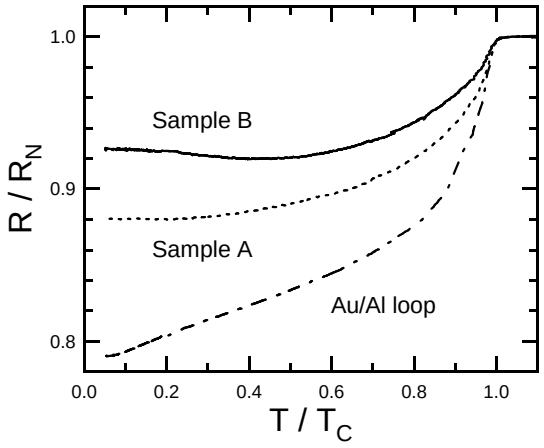

Fig. 3. Normalized resistance R/R_N for sample A, sample B, and the Au/Al loop structure as a function of temperature. R_N= 11.5 Ω, 5.0 Ω, and 10.0 Ω for sample A, sample B, and the Au/Al loop, respectively. T_c = 1.6 K for sample A, and 1.5 K for sample B and the Au/Al loop.

(70-ppm AuFe) control wire. The magnitude of T_K is comparable to the known values obtained from previous studies on a dilute-magnetic-impurity system of AuFe [14].

When a superconductor is in close contact with a dilute-magnetic-impurity system, the superconducting pair correlation is likely to penetrate beyond the interface. This superconducting proximity effect, which is sensitive to T, is expected to cause a continuous change of resistance at temperatures below T_c. Such a temperature dependence of the resistance was observed for both samples A and B, as shown in Figure 3. The normalized resistance in zero magnetic field begins to decrease rapidly as T is lowered below the T_c of the Al film. Since a part of the AuFe wire in samples A and B is shorted by the superconducting Al arm, the resistance drops rapidly just below T_c. For sample A, however, the resistance decreases progressively at a slower rate as T is further lowered, and finally the resistance begins to increase for $T \leq 0.35$ K. This non-monotonic temperature dependence is seen more clearly in the resistance of sample B. In Figure 3, we have also presented the resistance of the Au/Al loop of the same structure as sample B. In contrast to samples A and B, the resistance of the Au/Al loop continuously decreases down to the lowest temperature. The non-monotonic temperature dependences in the resistances of samples A and B are distinct from the reentrance observed in previous studies on normal metal/superconductor (N/S) proximity systems [15–18]. For the samples with a 4.7-μm length, a resistance minimum due to the reentrance is expected to occur at ∼10 mK (= E_c/k_B, where E_c is the Thouless energy), which is far below the lowest temperature in this experiment. Therefore, we believe that the non-monotonic temperature dependences in the resistances of samples A and B arise as the Kondo effect predominates over the superconducting proximity effect at low temperatures.

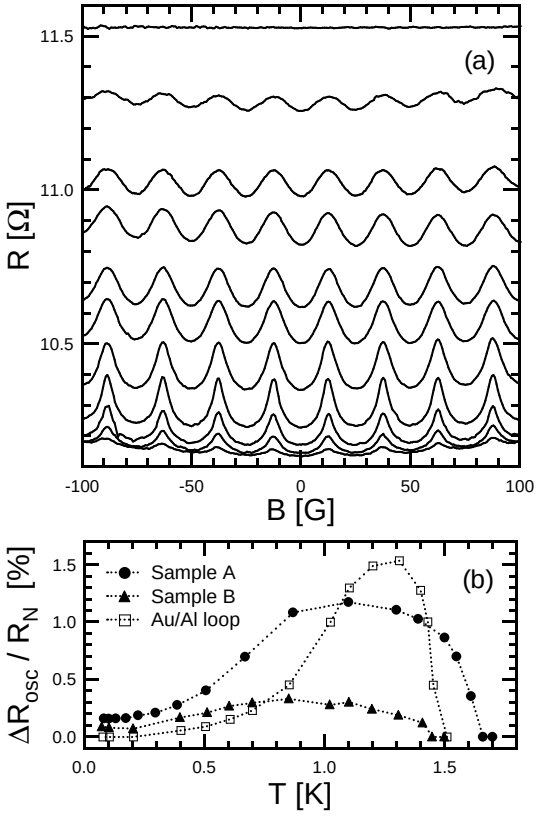

Fig. 4. (a) Magnetoresistance for sample A at T= 83 mK, 508 mK, 670 mK, 870 mK, 1.1 K, 1.3 K, 1.39 K, 1.5 K, 1.55 K, 1.61 K, and 1.66 K from bottom to top. (b) Normalized amplitudes of the magnetoresistance oscillation for sample A, sample B, and the Au/Al loop as a function of temperature.

The microscopic mechanism of the superconducting proximity effect is the Andreev reflection. Since an electron injected below the superconducting gap energy is Andreev-reflected with a phase memory of the superconducting condensate, the resistance of a normal metal wire between two N/S interfaces can be modulated by the macroscopic phase of the superconducting condensate [19]. An easy way to manipulate the phase is achieved by applying a magnetic field through the loop geometry. However, a prerequisite for the resistance modulation is phase coherence in the normal metal between the two N/S interfaces. Therefore, the magnetoresistance oscillation in the AuFe/Al hybrid loops provides direct evidence for phase coherent transport in Kondo AuFe wires. In Figure 4(a) the clear Aharonov-Bohm effect in the magnetoresistance of the hybrid loop (sample A) strongly suggests such evidence. The oscillation period of $\Delta B \approx 25.4$ G corresponds to the superconducting flux quantum, Φ_0 (= $h/2e$) divided by the loop area, which is equal to the area enclosed by the center of the hybrid loop ($\approx 0.80 \pm 0.01$ μm^2). A similar oscillation has been also observed in the magnetoresistance of sample B.

Figure 4(b) shows the amplitudes of the magnetoresis-

tance oscillations for samples A, B, and the Au/Al loop structure. The amplitude was determined by analyzing the power spectral density of the magnetoresistance oscillation between –100 G and +100 G. As the concentration of the magnetic impurity (Fe) increases, the maximum amplitude of the normalized magnetoresistance oscillation decreases. For proximity-induced metallic loops, the magnetoresistance oscillation increases as T is lowered and becomes largest when k_BT is of the order of the Thouless energy, $E_c = \hbar D/L^2$. Here, L is the length of the normal metal. At low T, the amplitude of the magnetoresistance oscillation shows a reentrant behavior and vanishes as $T \to 0$. This reentrant behavior originates from spatially nonuniform superconducting pair correlations in the normal metal under the proximity effect [20, 21]. The proximity-induced Cooper-pair amplitude is largest at the interface with a superconductor, whereas it vanishes at the contact with a normal reservoir. Such reentrant behavior was found in all the samples in this experiment. The amplitude of the magnetoresistance oscillation of the Au/Al loop showed the strongest reentrant behavior as it vanished completely below 200 mK. On the other hand, for samples A and B, the amplitudes showed relatively weak reentrant behavior. The amplitude remained finite even at the lowest temperature.

The reentrant temperature, T_m, can be estimated by using the relation $T_m \simeq E_c/k_B$. To estimate the reentrant temperature, however, one should be careful to correctly choose the normal metal length L. For the magnetoresistance oscillation, a suitable choice for L is the distance between the two N/S interfaces in the loop structure. By using $L \approx 0.5$ μm, T_m was estimated to be 0.9 K, 1.1 K, and 0.9 K, respectively, for sample A, sample B, and the Au/Al loop structure. Although rigorous estimates should include the contribution of the magnetic impurity, the estimate agrees with the results of measurements in Figure 4(b) to an order of magnitude.

The mesoscopic characteristic length scales that play an important role in this experiment are the thermal length L_T and the phase coherence length L_ϕ. L_T of the AuFe wires is estimated to be $\sim 0.47/\sqrt{T[K]}$ μm and $0.52/\sqrt{T[K]}$ μm for samples A and B, respectively, and $\sim 0.47/\sqrt{T[K]}$ μm for the Au/Al loop structure. Characterized by L_T, the range of the superconducting proximity effect already extends over the entire AuFe arm ($\sim$0.5 μm long) of the hybrid loop when the temperature reaches the T_c of the Al film. However, the superconducting proximity effect is also bounded by the single-electron phase coherence length, L_ϕ, which is affected by spin-flip scattering at the magnetic impurities. The Aharonov-Bohm effect in the magnetoresistance is disturbed as L_ϕ becomes shorter than the length of the normal arm of a hybrid loop.

Figure 5 shows L_ϕ of a meander-type 26-ppm AuFe control wire, which was estimated by using a weak localization measurement [22, 23]. The corresponding phase coherence time is shown in the inset of Figure 5. L_ϕ at

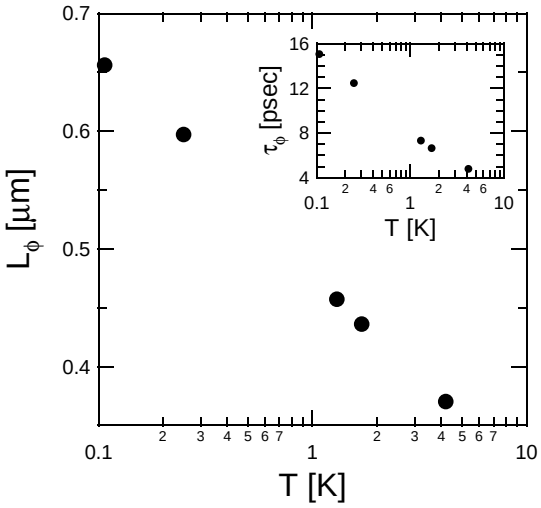

Fig. 5. Temperature dependence of the phase coherence length of the meander-type 26-ppm AuFe control wire. Inset: the phase coherence time of a meander-type 26-ppm AuFe control wire.

$T = 1.7$ K reaches 0.44 μm, which is comparable to the length of the normal arm of the hybrid loops. This is consistent with the existence of a magnetoresistance oscillation in the 26-ppm AuFe/Al hybrid loop. However, the maximum amplitudes of magnetoresistance oscillations are smaller for the samples with greater Fe concentrations because L_ϕ decreases with increasing Fe concentration. For comparison, we also obtained L_ϕ of a long Au control wire by using a weak localization measurement. L_ϕ of the pure Au wire at $T = 2.3$ K is 4.6 μm, which is an order of magnitude longer than that of the 26-ppm AuFe wire. Consequently, as Figure 4(b) shows, the maximum amplitude of the magnetoresistance oscillation is largest for the pure Au/Al hybrid loop.

III. CONCLUSIONS

In conclusion, our results confirm the existence of the superconducting proximity effect and electronic phase coherence in Kondo AuFe wires. The magnetoresistance oscillations of the AuFe/Al loops in this experiment support the previous work by Dikin *et al.*, in which the electron phase coherence length L_ϕ was the relevant length scale for Aharonov-Bohm magnetoresistance oscillations in proximity-coupled normal metals [24].

ACKNOWLEDGMENTS

We thank T.-S. Kim, H.-W. Lee, and V. Chandrasekhar for helpful discussions. This work was supported by the Korea Research Foundation Grant

funded by the Korean Government (MOEHRD) (KRF-2005-070-C00055) and by the SRC/ERC program of MOST/KOSEF (R11-2000-071).

REFERENCES

[1] H.-J. Lee, Y.-S. Shin, H.-M. So, J.-J. Kim, N. Kim and K.-H. Yoo, J. Korean Phys. Soc. **39**, 534 (2001).
[2] J. Eom, J. Korean Phys. Soc. **42**, L313 (2003).
[3] J. Eom, J. Aumentado, V. Chandrasekhar, P. M. Baldo and L. E. Rehn, Solid State Commun. **127**, 545 (2003).
[4] M. R. Buitelaar, T. Nussbaumer and C. Schönenberger, Phys. Rev. Lett. **89**, 256801 (2002).
[5] Y. Avishai, A. Golub and A. D. Zaikin, Phys. Rev. B **67**, 041301 (2003).
[6] M. Giroud, H. Courtois, K. Hasselbach, D. Mailly and B. Pannetier, Phys. Rev. B **58**, R11872 (1998).
[7] V. T. Petrashov, I. A. Sosnin, I. Cox, A. Parsons and C. Troadec, Phys. Rev. Lett. **83**, 3281 (1999).
[8] J. Aumentado and V. Chandrasekhar, Phys. Rev. B **64**, 54505 (2001).
[9] W. Belzig, A. Brataas, Y. V. Nazarov and G. E. W. Bauer, Phys. Rev. B **62**, 9726 (2000).
[10] F. S. Bergeret, A. F. Volkov and K. B. Efetov, Phys. Rev. Lett. **86**, 4096 (2001).
[11] The samples were implanted at a dose of 1.3×10^{13} (5.0×10^{13}) ions/cm^2 and an energy of 80 keV (100 keV) for the 26-ppm-Fe (70-ppm-Fe) concentration.
[12] The Fe concentration is estimated by using the slope of the Kondo resistance ($\sim$0.11 nΩcm/ppm decade K) for the AuFe data from J. Loram, P. J. Ford and T. E. Whall shown in A. J. Heeger, in *Solid State Physics*, Vol. 23, edited by H. Ehrenreich, F. Seitz and D. Turnbull (Academic Press, New York, 1969), p. 283.
[13] D. R. Hamann, Phys. Rev. **158**, 570 (1967).
[14] J. W. Loram, T. E. Whall and P. J. Ford, Phys. Rev. B **2**, 857 (1970); Phys. Rev. B **3**, 953 (1971).
[15] H. Courtois, Ph. Gandit and B. Pannetier, Phys. Rev. B **52**, 1162 (1995).
[16] H. Courtois1, Ph. Gandit, D. Mailly and B. Pannetier, Phys. Rev. Lett. **76**, 130 (1996).
[17] P. Charlat, H. Courtois, Ph. Gandit, D. Mailly, A. F. Volkov and B. Pannetier, Phys. Rev. Lett. **77**, 4950 (1996).
[18] C-J. Chien and V. Chandrasekhar, Phys. Rev. B **60**, 15356 (1999).
[19] M. Kim and J. Hong, J. Korean Phys. Soc. **46**, 689 (2005).
[20] Y. V. Nazarov and T. H. Stoof, Phys. Rev. Lett. **76**, 823 (1996).
[21] A. A. Golubov, F. K. Wilhelm and A. D. Zaikin, Phys. Rev. B **55**, 1123 (1997).
[22] P. Santhanam, S. Wind and D. E. Prober, Phys. Rev. B **35**, 3188 (1987).
[23] C. Van Haesendonck, J. Vranken and Y. Bruynseraede, Phys. Rev. Lett. **58**, 1968 (1987).
[24] D. A. Dikin, M. J. Black and V. Chandrasekhar, Phys. Rev. Lett. **87**, 187003 (2001).